Received: 5 May 2020 | Revised: 31 May 2020 | Accepted: 1 June 2020

DOI: 10.1002/ansa.202000053

ANALYTICAL SCIENCE ADVANCES

WILEY-VCH

FULL ARTICLE

# Rapid biomonitoring of perfluoroalkyl substance exposures in serum by multisegment injection-nonaqueous capillary electrophoresis-tandem mass spectrometry

**Sandi Azab**[1,2] | **Rebecca Hum**[1] | **Philip Britz-McKibbin**[1]

[1] Department of Chemistry and Chemical Biology, McMaster University, Hamilton, Ontario, Canada

[2] Department of Pharmacognosy, Alexandria University, Alexandria, Egypt

**Correspondence**
Department of Chemistry and Chemical Biology, McMaster University, Hamilton, ON, Canada.
Email: britz@mcmaster.ca

## Abstract

Perfluoroalkyl substances (PFASs) are a major contaminant class due to their ubiquitous prevalence, persistence, and putative endocrine disrupting activity that may contribute to chronic disease risk notably with exposures early in life. Herein, multisegment injection-nonaqueous capillary electrophoresis-tandem mass spectrometry (MSI-NACE-MS/MS) is introduced as a high throughput approach for PFAS screening in serum samples following a simple methyl-*tert*-butyl ether (MTBE) liquid extraction. Separation and ionization conditions were optimized to quantify low nanomolar concentration levels of perfluorooctanoic acid (PFOA) and perfluorooctanesulfonic acid (PFOS) from serum extracts when using multiple reaction monitoring under negative ion mode conditions. Multiplexed separations of PFOA and PFOS were achieved with excellent throughput (<3 min/sample), adequate concentration sensitivity (LOD ~ 20 nM, S/N = 3) and good technical precision over three consecutive days of analysis (mean CV = 9.1%, n = 84). Accurate quantification of PFASs was demonstrated in maternal serum samples (n = 16) when using MSI-CE-MS/MS following pre-column sample enrichment with median concentrations of 3.46 nM (0.7-9.0 nM) and 3.29 nM (1.5-6.6 nM) for PFOA and PFOS, respectively. This was lower than average PFAS exposures measured in pregnant women who had serum collected prior to 2009 likely due to subsequent phase out of their production. Overall, this method offers a convenient approach for large-scale biomonitoring of environmental exposures to legacy PFASs and their emerging replacements that is relevant to maternal health and chronic disease risk assessment in children.

KEYWORDS
capillary electrophoresis, mass spectrometry, maternal exposures, perfluoroalkyl substances, serum

## 1 | INTRODUCTION

Perfluoroalkyl substances (PFASs) are synthetic compounds first developed in the 1940s due to their unique thermal and chemical properties that render them useful in a myriad of consumer products and industrial applications.[1,2] These ubiquitous chemicals are both water and oil-repellant,

with heat-resistant and surface-active properties comprising over 4000 different perfluoroalkyl acid analogs.[3] PFASs have been incorporated in food packaging, electronics, stain-resistant textiles, non-stick coatings, as well as firefighting foams.[3-5] Yet, PFASs are a major contaminant class in environmental toxicology given their persistence and tendency to bioaccumulate with widespread human exposures from the ingestion of contaminated food and drinking water,[6,7] as well as household cookware, treated carpets, and waterproofed clothing.[8] Biomonitoring studies have largely focused on analyzing the two most abundant contaminants from this chemical class, namely perfluorooctanoic acid (PFOA) and perfluorooctanesulfonic acid (PFOS), which are classified as persistent organic pollutants (POPs) under the Stockholm Convention. With a global phase-out of PFOA and PFOS production with exceptions granted to certain products (e.g., medical devices), other alternatives have replaced these legacy contaminants, including short-chain (C4-C6) PFAS substitutes, and chlorinated polyfluoroalkyl ether sulfonic acids (Cl-PFESAs);[2,9] however, the long-term impacts of these emerging replacements for regulated PFASs on human and wildlife health remain poorly understood.[10] A study by the US Center for Disease Control and Prevention reported declining serum concentrations of PFOS in the population, constant levels of PFOA, and even increased concentrations of certain non-regulated PFASs (e.g., perfluorononanoic acid).[11] Long-range atmospheric and/or oceanic transport to polar regions with subsequent biotic uptake may explain these observations due to unregulated manufacturing and emission of PFASs occurring in developing countries.[12,13] For these reasons, there is urgent need for continued surveillance of PFASs as they are not effectively removed from wastewater treatment plants, which can also generate unexpected chlorinated by-products.[14]

Human exposure studies have shown that PFASs are predominately stored within the liver and in the circulation bound to plasma proteins with an estimated half-life ranging from 4 to 8 years.[3,15] As a result, blood is a specimen of choice for biomonitoring of PFAS exposures in the population.[16] Also, human breast milk represents a complementary specimen for assessment of PFAS exposures during infancy,[17] as well as urine that is correlated with PFAS levels in serum.[18] PFASs may function as potential endocrine disrupting chemicals due to their ability to compete with thyroxine binding to human thyroid hormone transport protein transthyretin[19] along with antagonist effects on receptors for testosterone[20] and progesterone.[21] Nevertheless, safe levels of PFAS exposures and their exact mechanisms of toxicity remain unclear[22] with health advisory limits of 0.07 µg/L PFOS and PFOA in drinking/ground water.[23] Similar to other environmental pollutants, children have a higher burden of PFASs as compared to adults,[24] attributed to transfer *in utero* from maternal exposures, feeding of breastmilk, and/or commercial baby formula,[25] and ingestion from active mouthing behavior that is exacerbated by indoor dust exposure.[26] Several studies have reported an inverse relation of PFOA and PFOS exposures to birth weight, as well as a direct relation to dyslipidemia and impaired gestational glucose homeostasis later in life.[4,27,28] In a study evaluating the association of maternal POPs serum levels with the risk of childhood obesity, PFOA and PFOS have been associated with increased BMI and risk for obesity in early childhood.[29] On the other hand, serum PFAS concentrations in children did not show a similar association, suggesting that exposure to environmental stressors *in utero* may represent a critical period of susceptibility during gestation.[29,30] Further research is needed to assess the long-term health impacts of early life exposures to PFASs and mixtures of other endocrine disrupting chemicals[31] using high throughput methods that enable low-cost and large-scale biomonitoring studies in environmental epidemiology.[32]

Analytical methods for PFAS determination require exquisite sensitivity and selectivity without complicated sample workup or background/matrix interferences.[33] Liquid chromatography coupled to tandem mass spectrometry (LC-MS/MS) with multiple reaction monitoring (MRM) is the gold standard for analysis of nanomolar levels of PFAS in complex biological and environmental samples.[16,34,35] Standardized protocols have been developed for reliable PFAS analysis by LC-MS/MS following pre-column sample enrichment and off-line clean-up using ion-pair extraction or anion-exchange solid-phase extraction (SPE).[34,36,37] Recent advances for PFAS screening by LC-MS/MS include on-line SPE with column switching to automate sample processing and reduce total analysis times (~28 min run/sample).[38] Capillary electrophoresis (CE) offers an alternative microseparation platform, but is far less commonly used for routine analysis of PFASs due to poor separation performance in aqueous buffer systems and/or inadequate concentration sensitivity and selectivity when using UV detection.[39–41] Recently, CE-MS using a novel nanospray interface was reported for anionic micropollutants analysis in drinking water samples, however deleterious peak broadening was noted for the surface-active contaminants, PFOA and PFOS.[42] Herein, we introduce a new strategy for high throughput screening of PFOA and PFOS in serum extracts when using multisegment injection-nonaqueous capillary electrophoresis-tandem mass spectrometry (MSI-NACE-MS/MS) following a simple methyl-*tert*-butyl (MTBE) extraction protocol.[43,44] Extensive method optimization and validation was performed to demonstrate reliable serum PFOA and PFOS analyses by MSI-NACE-MS/MS with stringent quality control (QC), which was applied to assess PFAS exposures in women during pregnancy as a pilot study.

## 2 | EXPERIMETAL SECTION

### 2.1 | Chemicals and reagents

Ultra LC-MS grade methanol (Caledon Inc., Georgetown, ON, Canada) and ultra LC-MS grade acetonitrile (Honeywell Inc., Muskegon, MI, USA) were used to prepare sheath liquid and background electrolyte (BGE), respectively. Ammonium acetate, ammonium hydroxide, butylated hydroxytoluene (BHT), methyl-*tert*-butyl ether (MTBE), PFOA and PFOS standards, chemicals, solvents, as well as standard human serum (S7023) used for initial

**TABLE 1** Optimized parameters for MSI-NACE-MS/MS determination of PFOS and PFOA with $^{13}C_8$-PFOS used as recovery standard in serum extracts

| Compound | MRM transition | Fragmentor Voltage (V) | Collision energy (V) | Cell accelerator voltage (V) | Dwell time (ms) |
|---|---|---|---|---|---|
| PFOS Quantifier | 499 → 80 | 60 | 60 | 5 | 100 |
| PFOS Qualifier | 499 → 99 | 60 | 60 | 5 | 200 |
| PFOA Quantifier | 413 → 369 | 60 | 10 | 7 | 100 |
| PFOA Qualifier | 413 → 169 | 60 | 10 | 7 | 100 |
| $^{13}C_8$-PFOS Quantifier | 507 → 80 | 60 | 60 | 5 | 100 |
| $^{13}C_8$-PFOS Qualifier | 507 → 99 | 60 | 60 | 5 | 200 |

optimization, were purchased from Sigma-Aldrich Inc. (St. Louis, MO, USA). The stable isotope sodium salt of perfluorooctanesulfonate ($^{13}C_8$.PFOS) was obtained from Cambridge Isotope Laboratories, Inc (Tewksbury, MA, USA).

## 2.2 | CE-MS instrumentation

An Agilent 6470 triple quadrupole (QQQ) mass spectrometer with a coaxial sheath liquid electrospray ionization (ESI) source coupled to an Agilent 7100 CE unit was used for all experiments (Agilent Technologies Inc., Mississauga, ON, Canada). An Agilent 1260 infinity isocratic pump with degasser were used to deliver a sheath liquid mixture of methanol:water (80:20 v/v) with 0.5% v/v $NH_4OH$ at a flow rate of 10 µL/min using a CE-MS coaxial sheath liquid interface kit. The nebulizing gas ($N_2$) was set off during serial sample injection and then turned on at a pressure of 10 psi during separation following voltage application.[43,44] The source capillary voltage (Vcap) was set at 3500 V with the drying gas at a flow rate of 4 L/min and the source temperature at 300°C in negative ion mode. For all PFAS standards, an MRM scan was performed including quantifier and qualifier ion transitions generated under optimal fragmentation voltages as summarized in Table 1. Separations were performed on bare fused-silica capillaries with 50 µm internal diameter, 360 µm outer diameter, and 90 cm total length (Polymicro Technologies Inc., AZ, USA). A capillary window maker (MicroSolv, Leland, NC, USA) was used to remove about 7 mm of the polyimide coating on both ends of the capillary to prevent polymer swelling when in contact with organic solvents.[45] The applied voltage was set to 30 kV at 25°C for CE separations together with a pressure application of 20 mbar (2 kPa) for the first 8 min followed by a 2 mbar/min gradient pressure increase. The nonaqueous background electrolyte (BGE) was composed of 35 mM of ammonium acetate in acetonitrile (70% v/v), methanol (15% v/v) and isopropanol (5% v/v) with an apparent pH of 9.5 adjusted by addition of 12% v/v of concentrated ammonium hydroxide. Samples were injected hydrodynamically at 50 mbar (5 kPa) alternating between 10 s for each sample plug and 40 s for the nonaqueous BGE spacer plug for a total of seven discrete samples analyzed within a single run. Prior to first use, capillaries were conditioned by flushing for 5 min at 950 mbar (95 kPa) sequentially with methanol, 0.1 M sodium hydroxide, deionized water, 1.0 M formic acid, deionized water then nonaqueous BGE for 15 min. Between runs, the capillary was flushed with nonaqueous BGE for 5 min at 950 mbar (95 kPa). Both nonaqueous BGE and sheath liquid solutions were degassed before use. Also, a chiller was used to circulate water at 4°C in the sample tray holder of the CE instrument to minimize evaporation of the nonaqueous BGE that was used up to four consecutive runs prior to its replacement.

## 2.3 | Calibration and method validation of MSI-NACE-MS/MS

Stock solutions (10 mM) of PFOA and PFOS calibrants were prepared in MTBE with addition of 0.1% w/v BHT as a neutral electroosmotic flow (EOF) marker. A serial dilution of calibrant solutions from 0.025 to 1.0 µM was prepared in triplicate when constructing seven-point calibration curves for PFASs using least-squares linear regression. All integrated peak areas for the quantifier ions were normalized using 1.0 µM $^{13}C_8$-PFOS as a stable-isotope internal standard. PFAS concentrations corresponding to limits of detection (LOD) and limits of quantification (LOQ) were calculated based on a serial dilution of calibrant solutions equivalent to a signal-to-noise ratio (SNR) of 3 and 10, respectively. Blank extracts were also prepared intermittently to confirm lack of sample carry-over effects and background interferences. Reproducibility was evaluated via intraday (n = 28) and interday (n = 84) precision studies based on three independent MSI-NACE-MS runs, at the beginning, middle, and end of day, each with seven replicate injections of a 1.0 µM PFAS calibrant mixture over three consecutive days. Method accuracy was assessed by spike-recovery studies using PFOA and PFOS standards at three different concentration levels (100, 500, 1000 nM) into standard human serum (Sigma S7023) prior to MTBE extraction. PFAS recovery was calculated based on the percentage difference between spiked and original (baseline) concentration of human serum divided by the spiked (known) concentration.

### 2.4 | Study birth cohorts

SouTh Asian birth cohoRT (START) study is a prospective birth cohort study involving 1006 predominantly South Asian pregnant women recruited from Brampton and Mississauga, Ontario between 2011 and 2015.[46] Fasting blood samples were collected in the second trimester, and serum was fractionated within 2 h from collection according to standard protocols and stored at −80°C. A subset of residual serum samples from START birth cohort (n = 16) were analyzed for PFOA and PFOS in this work. The Family Atherosclerosis Monitoring In earLY life (FAMILY) study is a prospective birth cohort study involving 839 predominantly white European pregnant women recruited from the greater Hamilton area between 2002 and 2009.[47] Fasting blood samples were collected in the second trimester, and serum was fractionated within 2 h from collection according to standard protocols and stored at −80°C. A pooled serum sample from FAMILY was used as a reference sample for PFAS analysis during method validation and was also used as a QC and introduced in every run to monitor technical precision when using MSI-NACE-MS/MS. Ethical approval and informed consent from all study participants were obtained.[46,47]

### 2.5 | Sample workup procedure for serum extracts

Human serum samples were prepared using a slightly modified extraction protocol using MTBE originally developed by Matyash *et al.*[44,48] First, 100 µL of 0.01% v/v BHT in methanol was mixed with a 200 µL aliquot of serum. Next, 500 µL of 0.01 µM $^{13}C_8$-PFOS in MTBE and 25 µL of 1.0 M HCl were added to the mixture followed by vigorous shaking for 30 min at room temperature. Phase separation was then induced by addition of 200 µL of deionized water. Samples were then centrifuged at 3000 × *g* at 4°C for 30 min to sediment protein at the bottom of the vial followed by a biphasic water and ether (top) layer. A fixed volume (400 µL) was collected from the upper MTBE layer into a new vial, then dried under a gentle stream of nitrogen gas at room temperature. Serum extracts were then stored at −80°C and reconstituted in 5.0 µL of acetonitrile/isopropanol/water (70:20:10 v/v/v) with 10 mM ammonium acetate prior to analysis. This extraction procedure results in an overall 40-fold enrichment of PFAS from serum with good quantitative recovery. Standard human serum samples (100 µL) were spiked with 100, 500, and 1000 nM PFAS in triplicates and extracted following the same protocol.

### 2.6 | Data processing and statistical analysis

MSI-NACE-MS data were analyzed using Agilent Mass Hunter Workstation Software (Qualitative Analysis, version B.06.00, Agilent Technologies Inc., 2012). Molecular features were extracted in profile mode using a 10 ppm mass window for all transitions. Extracted ion electropherograms (EIEs) were integrated after smoothing using a quadratic/cubic Savitzky-Golay function (15 points) and peak areas, migration times and SNR were transferred to Excel (Microsoft Office, Redmond, WA, USA) for calculation of relative integrated peak area (RPA), relative migration time (RMT), LOD, and LOQ. Least-squares linear regression analysis for external calibration curves and figures of merit calculations were performed using Excel. MedCalc version 12.5.0 (MedCalc Software, Ostend, Belgium) was used for generation of boxplots and control charts, and all extracted ion electropherograms were depicted using Igor Pro 5.0 software (Wavemetric Inc., Lake Oswego, OR, USA).

## 3 | RESULTS AND DISCUSSION

### 3.1 | Method optimization for PFAS analysis by MSI-NACE-MS/MS

Optimization of separation, ionization, and fragmentation conditions for PFASs was first explored when using MSI-NACE-MS/MS coupled to a coaxial sheath liquid interface (Figure 1A), which was recently validated for rapid quantification of serum fatty acids and accurate assessment of dietary fat intake.[43,44] In this case, multiplexed separations were performed using a serial hydrodynamic injection program involving the introduction of alternating sample and BGE segments within a bare fused-silica capillary to increase sample throughput without complicated column switching or hardware modifications.[49-51] However, perfluorinated anionic surfactants possess strong adsorption properties that contribute to band broadening and/or poor resolution in CE when using aqueous BGE conditions with inadequate organic modifier content.[42] As a result, a nonaqueous BGE system was used for separation of PFASs in this work, which was composed of 70% v/v acetonitrile, 15% v/v methanol, and 5% v/v isopropanol; however, residual water (10% v/v) was still needed for solubilization of ammonium acetate as the electrolyte (apparent pH of 9.5) to generate a stable current during electrophoretic separation. Figure 1B demonstrates a clear benefit of the nonaqueous BGE system as required for resolution of PFOS from PFOA unlike equivalent aqueous buffer conditions (pH 9.5) without organic modifiers that resulted in their co-migration after the EOF, where BHT serves as a neutral marker. In fact, baseline resolution of all seven independently introduced sample plugs in the same run was achieved

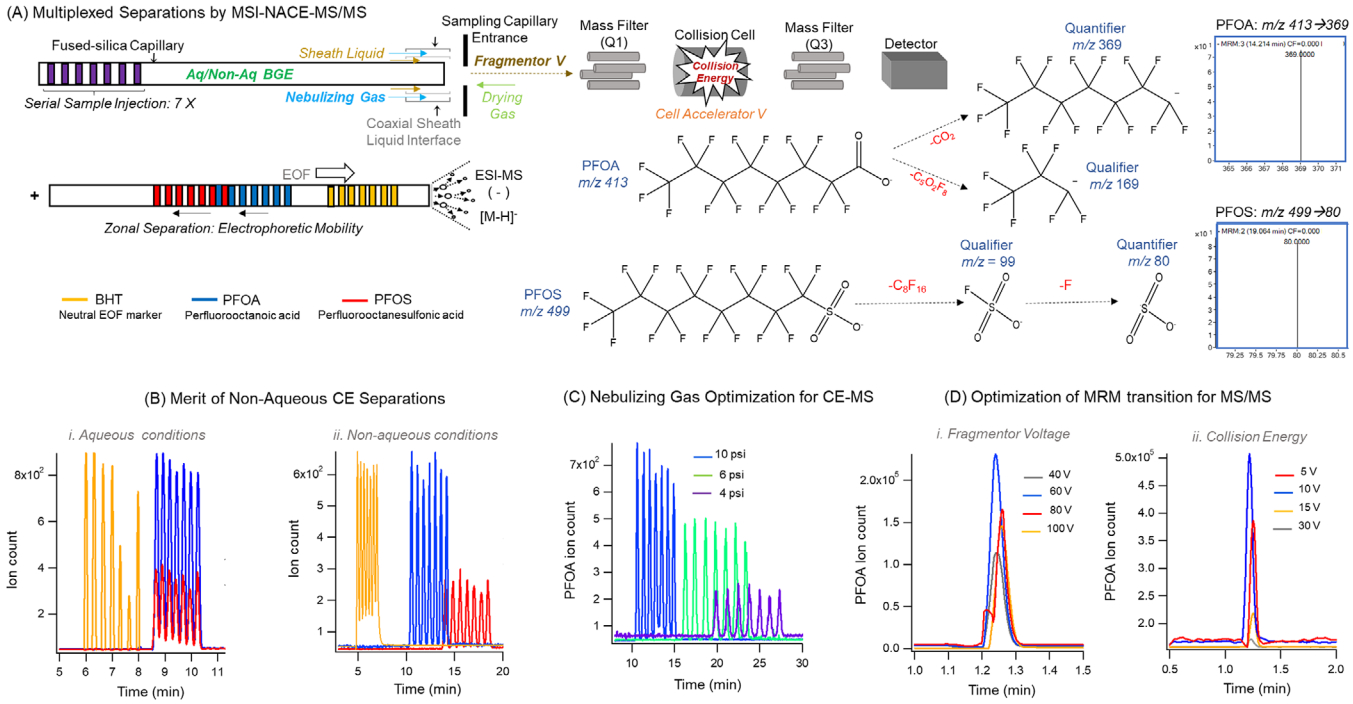


**FIGURE 1** A, Multiplexed separations of surface-active PFOA and PFOS when using MSI-NACE-MS based on serial injection of seven discrete samples followed by their zonal electrophoretic separation with MRM-scan data acquisition of quantifier (*m/z* 413 → 369 for PFOA *m/z* 499 → 80 for PFOS) and qualifier ions (*m/z* 413 → 169 for PFOA *m/z* 499 → 99 for PFOS) under negative ion mode detection. B, Comparison of PFOA and PFOS separation resolution under aqueous (left) and nonaqueous (right) background electrolyte conditions. C, Optimization of nebulizer gas pressure for the coaxial sheath liquid interface. D, Optimization of MRM transition parameters including fragmentor voltage (V) and collision energy for maximal precursor and product ion response, respectively

within 20 min (~3 min/sample) when using the nonaqueous BGE system with PFOS migrating with a larger apparent negative electrophoretic mobility (i.e., longer migration time) as compared to PFOA. Improved solubilization and specific solvent-solute interactions have long been attributed to the unique selectivity in NACE[52] with PFOS being bulkier, less volatile, and more hydrophobic than PFOA.[23] We recently demonstrated that a homologous series of fatty acids are accurately modeled in NACE based on their characteristic mobilities reflecting differences in carbon chain length and degree of unsaturation supporting their unambiguous identification complementary to high resolution MS.[43]

Other experimental variables also impacted PFAS separation performance, such as drying gas flow rate, nebulizer gas pressure, as well as a hydrodynamic pressure applied during electromigration (i.e., pressure-assisted NACE). Nebulizer gas pressure is required in the CE-MS interface to stabilize spray formation, and higher nebulizer gas velocities contributed to faster migration times due to a greater siphoning effect,[53] which in turn gave rise to sharper peaks and a threefold higher SNR as depicted for PFOA in Figure 1C. Nevertheless, the nebulizer gas was required to be shut off during serial sample introduction in MSI-NACE-MS/MS when using low viscosity nonaqueous BGE solutions that can give rise to suctioning of air within the capillary inlet resulting in a current drop upon voltage application.[43] In contrast, increasing drying gas flow rate from 4 to 8 L/min resulted in longer migration times exceeding 20 min for both PFOA and PFOS with greater band dispersion, whereas reducing it to 2 L/min shortened the separation window with insufficient resolution from the EOF. Next, a pressure gradient of 2 mbar/min starting at 8 min was also introduced to further sharpen peaks for improved resolution of PFASs while also reducing total analysis times. Lastly, selective yet sensitive analysis of PFASs was achieved by MSI-NACE-MS/MS when performing collisional-induced dissociation of precursor ions to generate characteristic product ions, including quantifier and qualifier ions that were detected via MRM as shown in Figure 1D. Table 1 summarizes optimal voltage settings for MRM transitions for quantifier and qualifier ions associated with PFOS, PFOA, and $^{13}C_8$-PFOS (as internal/recovery standard), including fragmentor voltage, cell accelerator voltage, and collision energy. A conventional electrospray ion source was optimal for MSI-NACE-MS/MS since it allowed for uninterrupted analyses without incidental capillary failures and/or current instabilities upon voltage application. In contrast, a dual Jet Stream electrospray source that uses a high flow of heated sheath gas together with a nozzle voltage was found to increase the susceptibility to corona discharge under negative ion mode conditions resulting in frequent capillary fractures.[43,45] Also, the Jet Stream electrospray source precludes the ability of the sheath gas to be turned off completely to avoid suctioning during sample introduction that is critical for stable runs when using nonaqueous BGE systems. As a result, systematic method optimization of several experimental variables in MSI-NACE-MS/MS was critical to enable high efficiency separation of PFASs with excellent selectivity, sensitivity, and robustness.

**TABLE 2** Method validation and figures of merit for rapid screening of PFOS and PFOA from serum extracts using MSI-NACE-MS/MS

| PFAS | Molecular Formula | RMT[a] | LOD[b] (nM) | LOQ[b] (nM) | Range[c] (nM) | Linearity[c] ($R^2$) | Mean % Recovery[d] | Intraday RMT[e] (CV) | Intraday RPA[e] (CV) | Interday RMT[e] (CV) | Interday RPA[e] (CV) |
|---|---|---|---|---|---|---|---|---|---|---|---|
| PFOA | $C_8HF_{15}O_2$ | 0.76 | 20 | 103 | 25-1000 | 0.997 | 97 ± 12 | 1.11 | 4.58 | 1.43 | 9.56 |
| PFOS | $C_8HF_{17}O_3S$ | 1.00 | 25 | 117 | 25-1000 | 0.995 | 109 ± 9 | 1.55 | 4.75 | 1.78 | 8.59 |

[a]Relative migration time (RMT) calculated by normalization to $^{13}C_8$-PFOS, which was also used for PFAS quantification based on relative peak area.
[b]LOD and LOQ were estimated at the lowest PFAS calibrant concentration that generated a SNR ≈ 3 and 10, respectively.
[c]Calibration curves from triplicate analysis of seven calibrant solutions for PFASs over a 40-fold concentration range normalized to C-PFOS.
[d]Average percentage recovery for PFASs was calculated based on the percentage difference between spiked and original concentrations (in normal human serum) divided by the spiked concentration with triplicate measurements performed (n = 3) at three concentration levels (100, 500, and 1000 nM).
[e]Precision was assessed by analyzing six replicate injections of 1.0 μM PFAS calibrants along with a blank at the beginning, middle and end of day, over three consecutive days analyzed using a single capillary. Method reproducibility determined by intraday (n = 28) and interday (n = 84) precision for both quantifier ions for PFOA and PFOS when using MSI-NACE-MS.

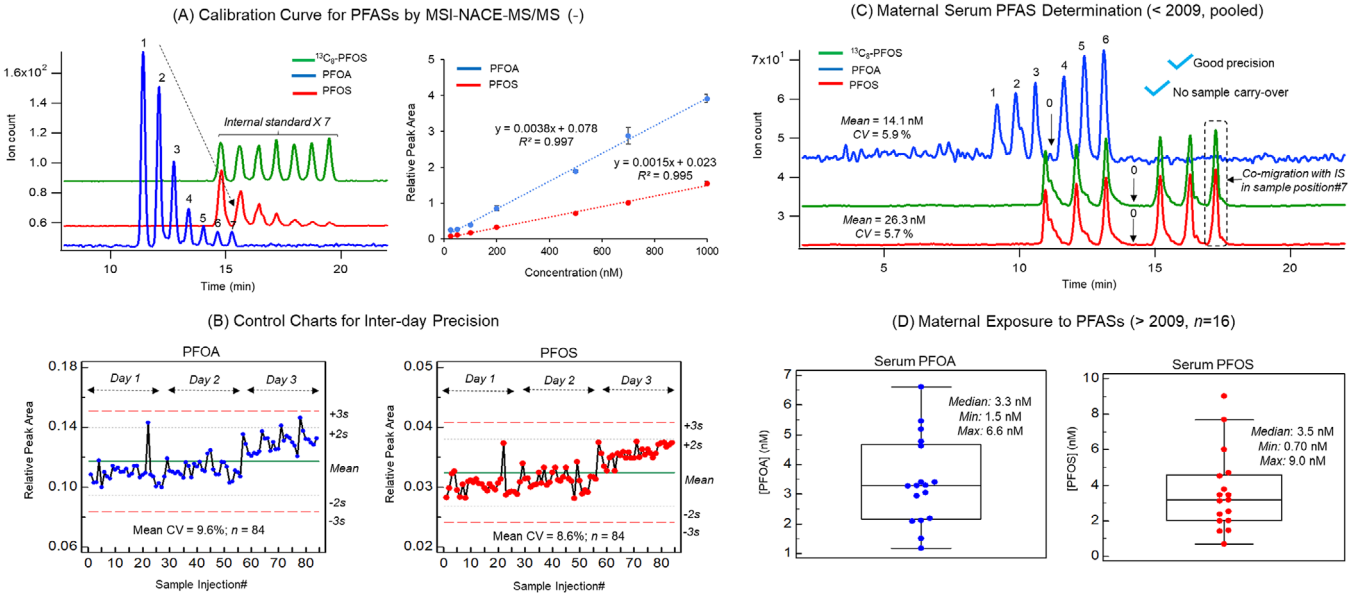


**FIGURE 2** A, Seven-point calibration curve for PFAS quantification by MSI-NACE-MS/MS over a 40-fold concentration range (25 to 1000 nM) based on their relative peak areas (RPA) normalized to $^{13}C_8$-PFOS (1000 nM) as a single stable-isotope internal standard. B, Control charts depicting long-term method precision over 3 days of analysis for a calibrant mixture (n = 84) of PFOA and PFOS when using MSI-NACE-MS/MS with mean CV < 10% and no outlier data exceeding action limits (±3 s). C, Method application on pooled maternal serum samples collected before 2009 from FAMILY highlighting higher PFAS exposures with precise measurements of six replicate serum extracts with no background signal in blank (0) extract. D, Boxplots showing the distribution of PFOA and PFOS serum concentrations in a subset of maternal serum samples (n = 16) from START collected after 2009

## 3.2 | Method validation for PFAS determination from serum extracts

Validation of the optimized MSI-NACE-MS/MS method was next performed for reliable quantification of PFOA and PFOS from serum extracts based on several figures of merit as summarized in Table 2. External calibration curves were generated based on triplicate analysis of seven calibrant solutions that were acquired in a single run from 25 to 1000 nM, each containing 1.0 μM $^{13}C_8$-PFOS as a single stable-isotope internal/recovery standard for peak area normalization to correct for variations in injection volume between samples as shown in Figure 2A. As expected, there is co-migration of $^{13}C_8$-PFOS and PFOS in all seven independently introduced sample plugs in MSI-NACE-MS/MS, which facilitates alignment and unambiguous confirmation of sample positions in cases when PFOS is not detected. Good linearity was acheived for PFOA and PFOS over a 40-fold linear dynamic range with correlation coefficients ($R^2$) of 0.997 and 0.995, respectively as highlighted in Figure 2A. The LOD (*SNR* ~ 3) and LOQ (*SNR* ~ 10) for PFOA were 20 nM and 102 nM, and for PFOS were 25 and 117 nM, respectively. As expected, these detection limits are considerably lower than previous CE methods coupled to UV detection (LOD ~ 3300 nM),[39] as well as NACE methods with online sample preconcentration using large-volume sample stacking or field-amplified sample injections (LOD ~ 30–280 nM).[41] Yet, LC-MS/MS methods with pre-column SPE reported significantly lower LODs for PFASs ranging from 0.02 to 0.20 nM due to the much larger sample volumes injected on-column (~100-fold) as com-

pared to CE (~10 nL).[34,38] For these reasons, off-line sample enrichment was critical to enable quantification of low nanomolar levels of PFOSs from serum extracts when using MSI-CE-MS/MS. In this case, a simple MTBE extraction protocol using a 200 µL serum aliquot was able to preconcentrate PFASs by a factor of 40-fold when reconstituted into 5.0 µL, which effectively reduced LOD and LOQ to about 0.5 and 2.5 nM, respectively. This compares well to a recent CE-MS method using a sheathless interface for analysis of trace levels of environmental contaminants with LOD of 0.1 and 0.8 nM reported for PFOA and PFOS, respectively.[42] Importantly, spike-recovery studies confirmed good method accuracy in standard human serum, which was performed in triplicate for PFOA and PFOS at three different concentration levels (100, 500, and 1000 nM). Overall, measured recoveries for PFASs in serum ranged from 86% to 123% with a mean recovery of 103% as summarized in Table 2. These results support the valid use of a single MTBE extraction fraction to ensure accurate quantification of PFASs that are predominately bound to human serum albumin in circulation, where PFOS has greater binding affinity than PFOA.[54] Lastly, assessment of both intraday (n = 28) and interday (n = 84) precision was performed by the analysis of a standard mixture of PFASs by MSI-NACE-MS/MS. Overall, the mean CV for the quantifier ions was 4.7% and 9.1% for intraday and interday precision, respectively, when responses were normalized to $^{13}C_8$-PFOS, whereas the mean CV for RMTs of PFOS and PFOA were <2.0% for 84 repeated injections (Table 2). Figure 2B depicts control charts for analysis of PFOA and PFOS highlighting acceptable long-term technical precision over 3 days of intermittent analyses (CV < 10%) with few outliers exceeding warning (±2 s), and no data exceeding action (±3 s) limits. As a result, high throughput screening of serum PFASs is feasible with acceptable accuracy, linearity, and precision when using MSI-NACE-MS/MS following a simple ether extraction procedure.

### 3.3 | Assessment of PFAS exposures in maternal serum

Following method optimization and validation, MSI-NACE-MS/MS was next applied to evaluate PFOS exposures in a sub-set of second trimester pregnant women (n = 16) from START. Additionally, a pooled maternal serum sample from FAMILY was used as a QC sample, as well as a reference comparator to evaluate potential changes in mean PFAS exposures prior to regulations to restrict PFAS production in 2009. Figure 2C shows representative extracted ion electropherograms for PFOA and PFOS detected from replicate serial injection of serum extracts for a pooled QC (n = 6) together with a blank extract (n = 1) when using MSI-NACE-MS/MS, which highlights good technical precision (CV < 6%) with no sample carryover effects/background contamination. Overall, pregnant women from FAMILY (collected prior to 2009) were found to have a higher average exposure of PFASs as compared to START (collected after 2009) with mean serum concentrations of PFOS and PFOA of 26 and 14 nM, respectively. In contrast, PFAS exposures assessed from individual pregnant women in START were variable yet much lower in concentration notably for PFOS, with median concentrations of 3.5 nM (range of 0.70-9.0 nM) and 3.3 nM (range of 1.5-6.6 nM) for PFOS and PFOA, respectively, as depicted in box-whisker plots in Figure 2D. These concentrations are consistent with exposures measured in a large cohort of Swedish women early in pregnancy with median concentrations of 10.8 and 3.9 nM for PFOS and PFOA, respectively, which also reported a higher risk for preeclampsia in women with greater PFAS exposures after adjustment for confounders.[55] Also, the lower PFAS exposures in START as compared to FAMILY is in agreement with longitudinal studies in the Fernald Community cohort that demonstrated decreasing serum concentration trajectories occurring from 2000 to 2008, especially for PFOS, yet with a corresponding increase in other unregulated PFAS analogs, such as perflourononanoic acid.[56] Future studies will investigate temporal changes in PFAS exposures in larger numbers of ethnically diverse birth cohorts, including assessing their impacts on childhood health outcomes. Also, the application of nanospray/sheathless interfaces in CE-MS[42,57] is needed to further lower detection limits under negative ion mode conditions for measurement of legacy PFASs and an expanding array of PFAS replacements relevant to contemporary exposures.

## 4 | CONCLUSION

PFASs pose an on-going challenge to environmental epidemiology due to their widespread pervasiveness and bioaccumulation that ensures a continued exposure risk given the rise of unregulated PFAS substitutes. For the first time, we demonstrate a rapid method for PFAS determination from serum when using MSI-NACE-MS/MS that is optimal for large-scale biomonitoring applications. This approach allows for reliable PFOS and PFOA quantification using a simple ether extraction protocol following rigorous method optimization and validation to ensure adequate robustness, accuracy, and precision. Our work overcomes previous technical challenges of CE/CE-MS methods using aqueous background electrolyte systems related to poor solubilization, deleterious band broadening and/or inadequate sensitivity for PFAS determination with low nanomolar detection limits. Multiplexed separations comprising seven or more discrete samples serially injected within a single run offers higher throughput (<3 min/sample) than conventional chromatographic separations with greater data fidelity since a reference sample and/or blank extract can be incorporated in each run for improved quality control and batch correction. Preliminary studies confirm that maternal exposures to PFOA and PFOS have largely decreased since 2009, with considerable between-subject variability in PFAS serum concentrations reflecting different exposure mechanisms in pregnant women. We anticipate that this method may allow for comprehensive PFAS surveillance when using full data acquisition with high resolution MS as required for elucidating the impact of early life exposures on the developmental origins of health and disease.

## ACKNOWLEDGMENTS

P.B.M. acknowledges funding from the Natural Sciences and Engineering Research Council of Canada, and Genome Canada. S.A. acknowledges funding from the Egyptian Ministry of Higher Education. Further thanks are extended to Dr. Sonia S. Anand, Dr. Koon K. Teo, Dr. Stephanie Atkinson, and other co-investigators from START and FAMILY cohorts for access to residual maternal serum used in the method application. We also acknowledge Marcus Kim and John Sausen from Agilent Technologies Inc. for helpful discussions, including loan of the triple quadrupole mass spectrometer.

## DATA AVAILABILITY STATEMENT

The data that support the findings of this study are available on request from the corresponding author. The data are not publicly available due to privacy or ethical restrictions.

## CONFLICT OF INTEREST

The authors declare no conflict of interest.

## ORCID

*Philip Britz-McKibbin* https://orcid.org/0000-0001-9296-3223

## REFERENCES

1. Houde M, Martin JW, Letcher RJ, Solomon KR, Muir DCG. Biological monitoring of polyfluoroalkyl substances: a review. *Environ Sci Technol*. 2006;40:3463-3473.
2. Wang Y, Shi Y, Vestergren R, Zhou Z, Liang Y, Cai Y. Using hair, nail and urine samples for human exposure assessment of legacy and emerging per- and polyfluoroalkyl substances. *Sci Total Environ*. 2018;636:383-391.
3. Lindstrom AB, Strynar MJ, Libelo EL. Polyfluorinated compounds: past, present, and future. *Environ Sci Technol*. 2011;45:7954-7961.
4. Wang Y, Zhang L, Teng Y, et al. Association of serum levels of perfluoroalkyl substances with gestational diabetes mellitus and postpartum blood glucose. *J Environ Sci*. 2018;69:5-11.
5. Dobraca D, Israel L, McNeel S, et al. Biomonitoring in California firefighters: metals and perfluorinated chemicals. *J Occup Environ Med*. 2015;57:88-97.
6. Trudel D, Horowitz L, Wormuth M, Scheringer M, Cousins IT, Hungerbühler K. Estimating consumer exposure to PFOS and PFOA. *Risk Anal*. 2008;28:251-269.
7. Trier X, Granby K, Christensen JH. Polyfluorinated surfactants (PFS) in paper and board coatings for food packaging. *Environ Sci Pollut Res*. 2011;18:1108-1120.
8. Domazet SL, Grøntved A, Timmermann AG, Nielsen F, Jensen TK. Longitudinal associations of exposure to perfluoroalkylated substances in childhood and adolescence and indicators of adiposity and glucose metabolism 6 and 12 years later: the European youth heart study. *Diabetes Care*. 2016;39:1745-1751.
9. Jian J-M, Chen D, Han F-J, et al. A short review on human exposure to and tissue distribution of per- and polyfluoroalkyl substances (PFASs). *Sci Total Environ*. 2018;636:1058-1069.
10. Liu Y, Ruan T, Lin Y, et al. Chlorinated polyfluoroalkyl ether sulfonic acids in marine organisms from Bohai Sea, China: occurrence, temporal variations, and trophic transfer behavior. *Environ Sci Technol*. 2017;51:4407-4414.
11. Kato K, Wong L-Y, Jia LT, Kuklenyik Z, Calafat AM. Trends in exposure to polyfluoroalkyl chemicals in the U.S. population: 1999–2008†. *Environ Sci Technol*. 2011;45:8037-8045.
12. Zhao Z, Xie Z, Möller A, et al. Distribution and long-range transport of polyfluoroalkyl substances in the Arctic, Atlantic Ocean and Antarctic Coast. *Environ Pollut*. 2012;170:71-77.
13. Yeung LWY, Dassuncao C, Mabury S, Sunderland EM, Zhang X, Lohmann R. Vertical profiles, sources, and transport of PFASs in the Arctic ocean. *Environ Sci Technol*. 2017;51:6735-6744.
14. Wang Y, Yu N, Zhu X, et al. Suspect and nontarget screening of per- and polyfluoroalkyl substances in wastewater from a fluorochemical manufacturing park. *Environ Sci Technol*. 2018;52:11007-11016.
15. Olsen GW, Burris JM, Ehresman DJ, et al. Half-life of serum elimination of perfluorooctanesulfonate, perfluorohexanesulfonate, and perfluorooctanoate in retired fluorochemical production workers. *Environ Health Perspect*. 2007;115:1298-1305.
16. Haug LS, Thomsen C, Becher G. A sensitive method for determination of a broad range of perfluorinated compounds in serum suitable for large-scale human biomonitoring. *J Chromatogr A*. 2009;1216:385-393.
17. Kärrman A, Ericson I, van Bavel B, etal. Exposure of perfluorinated chemicals through lactation: levels of matched human milk and serum and a temporal trend, 1996-2004, in Sweden. *Environ Health Perspect*. 2007;115:226-230.
18. Worley RR, Moore SM, Tierney BC, et al. Per- and polyfluoroalkyl substances in human serum and urine samples from a residentially exposed community. *Environ Int*. 2017;106:135-143.
19. Kar S, Sepúlveda MS, Roy K, Leszczynski J. Endocrine-disrupting activity of per- and polyfluoroalkyl substances: exploring combined approaches of ligand and structure based modeling. *Chemosphere*. 2017;184:514-523.
20. Di Nisio A, Sabovic I, Valente U, et al. Endocrine disruption of androgenic activity by perfluoroalkyl substances: clinical and experimental evidence. *J Clin Endocrinol Metab*. 2019;104:1259-1271.
21. Di Nisio A, Rocca MS, Sabovic I, et al. Perfluorooctanoic acid alters progesterone activity in human endometrial cells and induces reproductive alterations in young women. *Chemosphere*. 2020;242:125208.
22. Kotthoff M, Bücking M. Four chemical trends will shape the next decade's directions in perfluoroalkyl and polyfluoroalkyl substances research. *Front Chem*. 2018;6:103.

23. Viberg H, Eriksson P. Perfluorooctane sulfonate (PFOS) and perfluorooctanoic acid (PFOA). In: RC Gupta, ed., *Reproductive and Developmental Toxicology*. Cambridge, MA: Academic Press; 2011:623-635.
24. Koponen J, Winkens K, Airaksinen R, et al. Longitudinal trends of per- and polyfluoroalkyl substances in children's serum. *Environ Int*. 2018;121:591-599.
25. Llorca M, Farré M, Picó Y, Teijón ML, Álvarez JG, Barceló D. Infant exposure of perfluorinated compounds: levels in breast milk and commercial baby food. *Environ Int*. 2010;36:584-592.
26. Winkens K, Giovanoulis G, Koponen J, et al. Perfluoroalkyl acids and their precursors in floor dust of children's bedrooms – implications for indoor exposure. *Environ Int*. 2018;119:493-502.
27. Uppal JS, Zheng Q, Le XC. Maternal exposure to specific perfluoroalkyl substances is associated with increasing blood glucose in pregnant women. *J Environ Sci*. 2018;69:1-2.
28. Sunderland EM, Hu XC, Dassuncao C, Tokranov AK, Wagner CC, Allen JG. A review of the pathways of human exposure to poly- and perfluoroalkyl substances (PFASs) and present understanding of health effects. *J Expo Sci Environ Epidemiol*. 2019;29:131-147.
29. Karlsen M, Grandjean P, Weihe P, Steuerwald U, Oulhote Y, Valvi D. Early-life exposures to persistent organic pollutants in relation to overweight in preschool children. *Reprod Toxicol*. 2017;68:145-153.
30. Wang Y, Han W, Wang C, et al. Efficiency of maternal-fetal transfer of perfluoroalkyl and polyfluoroalkyl substances. *Environ Sci Pollut Res*. 2019;26:2691-2698.
31. Nadal A, Quesada I, Tudurí E, Nogueiras R, Alonso-Magdalena P. Endocrine-disrupting chemicals and the regulation of energy balance. *Nat Rev Endocrinol*. 2017;13:536-546.
32. Heindel JJ, Skalla LA, Joubert BR, Dilworth CH, Gray KA. Review of developmental origins of health and disease publications in environmental epidemiology. *Reprod Toxicol*. 2017;68:34-48.
33. Barceló D, Ruan T. Challenges and perspectives on the analysis of traditional perfluoroalkyl substances and emerging alternatives. *TrAC Trends Anal Chem*. 2019;121:115605.
34. Nakayama SF, Isobe T, Iwai-Shimada M, et al. Poly- and perfluoroalkyl substances in maternal serum: method development and application in pilot study of the Japan environment and children's study. *J Chromatogr A*. 2020.
35. Trojanowicz M, Koc M. Recent developments in methods for analysis of perfluorinated persistent pollutants. *Microchim Acta*. 2013;180:957-971.
36. Onghena M, Moliner-Martinez Y, Picó Y, Campíns-Falcó P, Barceló D. Analysis of 18 perfluorinated compounds in river waters: comparison of high performance liquid chromatography–tandem mass spectrometry, ultra-high-performance liquid chromatography–tandem mass spectrometry and capillary liquid chromatography–mass spectrometry. *J Chromatogr A*. 2012;1244:88-97.
37. Keller JM, Calafat AM, Kato K, et al. Determination of perfluorinated alkyl acid concentrations in human serum and milk standard reference materials. *Anal Bioanal Chem*. 2010;397:439-451.
38. Poothong S, Lundanes E, Thomsen C, Haug LS. High throughput online solid phase extraction-ultra high performance liquid chromatography-tandem mass spectrometry method for polyfluoroalkyl phosphate esters, perfluoroalkyl phosphonates, and other perfluoroalkyl substances in human serum, plasma, and whole blood. *Anal Chim Acta*. 2017;957:10-19.
39. Wójcik L, Szostek B, Maruszak W, Trojanowicz M. Separation of perfluorocarboxylic acids using capillary electrophoresis with UV detection. *Electrophoresis*. 2005;26:1080-1088.
40. Wójcik L, Korczak K, Szostek B, Trojanowicz M. Separation and determination of perfluorinated carboxylic acids using capillary zone electrophoresis with indirect photometric detection. *J Chromatogr A*. 2006;1128:290-297.
41. Knob R, Maier V, Petr J, Ranc V, Ševčík J. On-line preconcentration of perfluorooctanoic acid and perfluorooctanesulfonic acid by nonaqueous capillary electrophoresis. *Electrophoresis*. 2012;33:2159-2166.
42. Höcker O, Bader T, Schmidt TC, Schulz W, Neusüß C. Enrichment-free analysis of anionic micropollutants in the sub-ppb range in drinking water by capillary electrophoresis-high resolution mass spectrometry. *Anal Bioanal Chem*. 2020. https://doi.org/10.1007/s00216-020-02525-8
43. Azab S, Ly R, Britz-McKibbin P. Robust method for high-throughput screening of fatty acids by multisegment injection-nonaqueous capillary electrophoresis–mass spectrometry with stringent quality control. *Anal Chem*. 2019;91:2329-2336.
44. Azab SM, de Souza RJ, Teo KK, etal. Serum non-esterified fatty acids have utility as dietary biomarkers of fat intake from fish, fish oil and dairy in women. *J Lipid Res*. 2020;61:933–944.
45. Yamamoto M, Ly R, Gill B, Zhu Y, Moran-Mirabal J, Britz-McKibbin P. Robust and high-throughput method for anionic metabolite profiling: preventing polyimide aminolysis and capillary breakages under alkaline conditions in capillary electrophoresis-mass spectrometry. *Anal Chem*. 2016;88:10710-10719.
46. Anand SS, Gupta M, Teo KK, et al. Causes and consequences of gestational diabetes in South Asians living in Canada: results from a prospective cohort study. *CMAJ Open*. 2017;5:E604-E611.
47. Morrison KM, Atkinson SA, Yusuf S, et al. The family atherosclerosis monitoring in early life (FAMILY) study. *Am Heart J*. 2009;158:533-539.
48. Matyash V, Liebisch G, Kurzchalia TV, Shevchenko A, Schwudke D. Lipid extraction by methyl- *tert* -butyl ether for high-throughput lipidomics. *J Lipid Res*. 2008;49:1137-1146.
49. Kuehnbaum NL, Kormendi A, Britz-McKibbin P. Multisegment injection-capillary electrophoresis-mass spectrometry: a high-throughput platform for metabolomics with high data fidelity. *Anal Chem*. 2013;85:10664-10669.
50. DiBattista A, Rampersaud D, Lee H, Kim M, Britz-McKibbin P. High throughput screening method for systematic surveillance of drugs of abuse by multisegment injection–capillary electrophoresis–mass spectrometry. *Anal Chem*. 2017;89:11853-11861.
51. Shanmuganathan M, Macklai S, Barrenas Cárdenas C, et al. High-throughput and comprehensive drug surveillance using multisegment injection-capillary electrophoresis mass spectrometry. *J Vis Exp*. 2019;(146):58986.
52. Kenndler E. A critical overview of non-aqueous capillary electrophoresis. Part I: mobility and separation selectivity. *J Chromatogr A*. 2014;1335:16-30.
53. Huikko K, Kotiaho T, Kostiainen R. Effects of nebulizing and drying gas flow on capillary electrophoresis/mass spectrometry. *Rapid Commun Mass Spectrom*. 2002;16:1562-1568.
54. Chi Q, Li Z, Huang J, Ma J, Wang X. Interactions of perfluorooctanoic acid and perfluorooctanesulfonic acid with serum albumins by native mass spectrometry, fluorescence and molecular docking. *Chemosphere*. 2018;198:442-449.
55. Wikström S, Lindh CH, Shu H, Bornehag C-G. Early pregnancy serum levels of perfluoroalkyl substances and risk of preeclampsia in Swedish women. *Sci Rep*. 2019;9:9179.

56. Blake BE, Pinney SM, Hines EP, Fenton SE, Ferguson KK. Associations between longitudinal serum perfluoroalkyl substance (PFAS) levels and measures of thyroid hormone, kidney function, and body mass index in the Fernald Community Cohort. *Environ Pollut*. 2018;242:894-904.
57. Lin L, Liu X, Zhang F, et al. Analysis of heparin oligosaccharides by capillary electrophoresis-negative-ion electrospray ionization mass spectrometry. *Anal Bioanal Chem*. 2017;409:411-420.

**How to cite this article:** Azab S, Hum R, Britz-McKibbin P. Rapid biomonitoring of perfluoroalkyl substance exposures in serum by multisegment injection-nonaqueous capillary electrophoresis-tandem mass spectrometry. *Anal Sci Adv*. 2020;1:173–182.
https://doi.org/10.1002/ansa.202000053